Influence of climate variability, fire and phosphorus limitation on the vegetation structure and dynamics in the Amazon-Cerrado border

Emily Ane Dionizio da Silva[1], Marcos Heil Costa[1], Andrea Almeida Castanho[2], Gabrielle Ferreira Pires[1], Beatriz Schwantes Marimon[3], Ben Hur Marimon-Junior[3], Eddie Lenza[3], Fernando Martins Pimenta[1], Xiaojuan Yang[4], Atul K. Jain[5]

[1] Department of Agricultural Engineering, Federal University of Viçosa (UFV), Viçosa, MG, Brazil

[2] The Woods Hole Research Center, 149 Woods Hole Rd., Falmouth, MA USA

[3] Federal University of Mato Grosso, Nova Xavantina Campus, Nova Xavantina, MT, Brazil

[4] Oak Ridge National Laboratory, Oak Ridge, TN, USA

[5] Department of Atmospheric Sciences, University of Illinois at Urbana-Champaign

Correspondence to: Emily Ane D. da Silva (emilyy.ane@gmail.com)

Abstract

17   Climate, fire and soil nutritional limitation are important elements that affect the vegetation

18 dynamics in areas of forest-savanna transition. In this paper, we use the dynamic vegetation model

19 INLAND to evaluate the influence of inter-annual climate variability, fire and phosphorus (P) limitation

20 on the Amazon-Cerrado transitional vegetation structure and dynamics. We assess how each

21 environmental factor affects the net primary production, leaf area index and aboveground biomass (AGB),

22 and compare the AGB simulations of observed AGB map. We used two regional datasets − the 1961-

23 1990average seasonal climate and the 1948 to 2008 inter-annual climate variability, two datasets of total

24 soil P content in soil, based on regional (field measurements) and global data and the INLAND fire

25 module. Our results show that inter-annual climate variability, P limitation and fire occurrence gradually

26 improve simulated vegetation types and these effects are not homogeneous along the

27 latitudinal/longitudinal gradient showing a synergistic effect among them. In terms of magnitude, the

28 effect of fire is stronger, and is the main driver of vegetation changes along the transition. The nutritional

29 limitation, in turn, is stronger than the effect of inter-annual climate variability acting on the transitional

30 ecosystems dynamics. Overall, INLAND typically simulates more than 80% of the AGB variability in

31 the transition zone. However, the AGB in many places is clearly not well simulated, indicating that

32 important soil and physiological factors in the Amazon-Cerrado border, such as lithology and water table

33 depth, carbon allocation strategies and mortality rates, still need to be included in the model.

1   Introduction

The Amazon and Cerrado are the two largest and most important phytogeographical domains in South America. The Amazon forest has been globally recognized and distinguished not only for its exuberance in diversity and species richness, but also for playing an important role in the global climate by regulating water (Bonan, 2008; Pires and Costa, 2013) and heat fluxes (Shukla et al., 1990; Rocha et al., 2004; Roy et al., 2002). The Cerrado is recognized worldwide for being the richest savanna in the world (Myers et al., 2000; Klink and Machado, 2005). It is characterized by different physiognomies, ranging from sparse physiognomies to dense woodland formations, and the latter are commonly mixed with Amazon rainforest forming transitional areas. The Amazon-Cerrado transition extends for 6270 km from northeast to southwest in Brazil, and the ecotonal vegetation around this transition is a mix of the characteristics of the tropical forest and the savanna (Torello-Raventos et al., 2013).

Gradients of seasonal rainfall and water deficit, fire occurrence, herbivory and low fertility of the soil have been reported as the main factors that characterize the transition between forest and savanna globally (Lehmann et al., 2011; Hoffman et al., 2012; Murphy and Bowman, 2012). However, few studies have evaluated the individual and combined effects of these factors on Brazilian ecosystems ecotones (Marimon-Junior and Haridasan, 2005; Elias et al., 2013; Vourtilis et al., 2013).

It is challenging to assess the degree of interaction among these various environmental factors in the transitional region and to infer how each one influences the distribution of the regional vegetation. In this case, Dynamic Global Vegetation Models (DGVMs) can be powerful tools to isolate the influences of climate, fire and nutrients, therefore helping to understand their large-scale effects on vegetation (House et al., 2003; Favier et al., 2004; Hirota et al., 2010; Hoffman et al., 2012).

55   Previous modelling studies using DGVMs that investigate climate effects in the Amazon indicate

56   that the rainforest could experience changes in rainfall patterns which would either transform the forest

57   into an ecosystem with more sparse vegetation – similar to a savanna, what has been called as the

58   "savannization of the Amazon" (Shukla et al., 1990; Cox et al., 2000; Oyama and Nobre, 2003; Betts et

59   al., 2004; Cox et al., 2004; Salazar et al., 2007) - or to a seasonal forest (Malhi et al., 2009; Pereira et al.,

60   2012; Pires and Costa, 2013). These studies had great importance to the improvement of terrestrial

61   biosphere modeling, but they neglect two important processes in tropical ecosystem dynamics: fire

62   occurrence and nutrient limitation, particularly the Phosphorus (P) limitation.

63   In tropical ecosystems, fire plays an important ecological role and influences the productivity, the

64   biogeochemical cycles and the dynamics in the transitional biomes, not only by changing the phenology

65   and physiology of plants, but also by modifying the competition among trees and lower canopy plants

66   such as grasses, shrubs and lianas. Fire occurrence, depending on its frequency and intensity, may increase

67   the mortality of trees and transform an undisturbed forest into a disturbed and flammable one (House et

68   al., 2003; Hirota et al., 2010; Hoffmann et al., 2012). Fires also affect the dynamics of nutrients in the

69   savanna ecosystem, changing mainly the N:P relationship and P availability in the soil (Nardoto et al.

70   2006).

71   Studies suggest that P is the main limiting nutrient within tropical forests (Malhi et al., 2009;

72   Mercado et al., 2011; Quesada et al., 2012) unlike the temperate forests. Phosphorus is a nutrient that is

73   easily adsorvided by soil minerals due to the large amount of iron and aluminum oxides in the Amazon

74   and Cerrado acidic and strongly weathered soils (Dajoz, 2005; Goedert, 1986). In the tropics, the warm

75   and wet climate favors the high biological activity in the soil and the litter decomposition, not limiting

the nitrogen for plant fixation. In Cerrado, higher soil fertility is related to regions with greater woody plants abundance and less grass cover, similarly to the features found in the Amazon rainforest (Moreno et al., 2008; Vourtilis et al., 2013; Veenendaal et al., 2015). However, the phosphorus limitation is often neglected by DGVMs. which usually assume unlimited P availability and consider nitrogen as the main limiting nutrient. However, N is not a limiting nutrient for trees in the tropics (Davidson et al. 2004), while P availability affects the trees dynamics.

In principle, in transitional forests, where the climate is intermediate between wet and seasonally dry, the heterogeneous structure and phenology make it difficult to represent these forests in models. The Amazon-Cerrado border is the result of the expansion and contraction of the Cerrado into the forest (see Marimon et al., 2006; Morandi et al., 2016), especially in the Mato Grosso state, where extreme events, such as intense droughts, influence the vegetation dynamics (Marimon et al., 2014) and the nutrient (Oliveira et al., 2017) and carbon cycling (Valadão et al., 2016).

Currently, no model has demonstrated to be able to accurately simulate the vegetation transition between Amazon and Cerrado. In general the DGVMs simulate evergreen forest along the Amazon-Cerrado border and neglect savanna occurrence (Botta and Foley, 2002; Bond et al., 2005; Salazar et al., 2007; Smith et al., 2014). This difficulty may be due to absence or not well represented disturbances such as fire, nutritional limitation or soil proprieties. Thus, we need a better understanding of the drivers on transitional vegetation to determine the parameters and establish relations between the environmental and transitional vegetation physiognomies.

In this paper we use the dynamic vegetation model INLAND (Integrated Model of Land Surface Processes) to evaluate the influence of inter-annual climate variability, fire occurrence and P limitation

97 in the Amazon-Cerrado transitional vegetation dynamics and structure. We assess how each element

98 affects the net primary production (NPP), leaf area index (LAI) and aboveground biomass (AGB) and

99 compare the model simulated AGB to observed AGB data. The results presented here are important to

100 build models that accurately represent the transition vegetation, and show the need to include the spatial

101 variability of eco-physiological parameters in these areas.

102 **2   Materials and methods**

103 **2.1   Study Area**

104   The present study focuses on the Amazon-Cerrado transition (Figure 1). We use the official

105 delimitation of the Brazilian biomes proposed by IBGE (2004), and define five transects along the

106 transition border with $1° \times 1°$ grid size (the terms "transition", "Amazon-Cerrado transition" and "Forest-

107 Savanna transition" are used interchangeably with the same meaning throughout this

108 manuscript).Transects 1 to 4 are established considering approximately 330 km into the Amazon and 330

109 km into the Cerrado domain, while Transect 5 is 880 km long on the southern Amazon-Cerrado border.

110 The transects are located as follows: Transect 1 (T1, 44°- 50°W; 5°- 7°S), Transect 2 (T2, 46°-51° W; 7°-

111 9S), Transect 3 (T3, 48°-54° W; 9°-11° S), Transect 4 (T4, 49° - 55° W; 11°-13° S), and Transect 5 (T5,

112 52° - 60° W; 13°-15° S) (Figure 1).

113 **2.2   Description of the INLAND Surface Model**

114   The Integrated Model of Land Surface Processes (INLAND) is the land-surface component of the

115 Brazilian Earth System Model (BESM). INLAND is basically a revision of the IBIS model (Integrated

116 Biosphere Simulator, described by Foley et al., 1996; Kucharik et al., 2000), through assembly and

117 standardization of different IBIS versions, and improvements in software engineering. We used the

118 version described by Senna et al. (2009) as starting point for INLAND. No changes in tuning were done

119 since that paper, except the addition of the P parameterization, described below. Code is available from

120 http://www.biosfera.dea.ufv.br/en-US/download-inland.

121   The model considers changes in the composition and structure of vegetation in response to the

122 environment and incorporates important aspects of biosphere-atmosphere interactions. The model

123 simulates the exchanges of energy, water, carbon and momentum between soil-vegetation-atmosphere.

124 These processes are organized in a hierarchical framework and operate at different time steps, ranging

125 from 60 minutes to 1 year, coupling ecological, biophysical and physiological processes. The vegetation

126 structure is represented by two layers: upper (arboreal PFTs) and lower (no arboreal PFTs, shrubs and

127 grasses) canopies, and the composition is represented by 12 plant functional types (PFTs) (e.g., tropical

128 broadleaf evergreen trees or C4 grasses, among several others).The photosynthesis and respiration

129 processes are simulated in a mechanistic manner using the Ball-Berry-Farquhar model (details in Foley

130 et al., 1996). The vegetation phenology module simulates the processes such as budding and senescence

131 based on drought phenology scheme for tropical deciduous trees. The dynamic vegetation module

132 computes the following variables yearly for each PFT: gross and net primary productivity (GPP and NPP),

133 changes in AGB pools, simple mortality disturbance processes and resultant LAI, thus allowing

134 vegetation type and cover to change with time. The partitioning of the NPP for each PFT resolves carbon

135 in three AGB pools: leaves, stems and fine roots. The LAI of each PFT is obtained by simply dividing

136 leaf carbon by specific leaf area, which in INLAND is considered fixed (one value) for each PFT.

137   INLAND has eight soil layers to simulate the diurnal and seasonal variations of heat and moisture.

138   Each layer is described in terms of soil temperature, volumetric water content and ice content (Foley et

139   al., 1996; Thompson and Pollard, 1995). Furthermore, all of these processes are influenced by soil texture

140   and amount of organic matter within the soil profile.

141   Considering these aspects of vegetation dynamics and soil physical properties the model can

142   simulate plant competition for light and water between trees, shrubs and grasses through shading and

143   differences in water uptake (Foley et al., 1996). These PFTs can coexist within a grid cell and their annual

144   LAI values indicate the dominant vegetation type within a grid cell. For example, the dominant vegetation

145   type is a Tropical Evergreen Forest if the PFT tropical broadleaf evergreen tree has an annual mean upper

146   canopy LAI (LAI_{upper}) above 2.5 m^2 m^{-2}. On the other hand, the dominant vegetation type is a Tropical

147   Deciduous Forest if the tropical broadleaf drought-deciduous tree has an annual mean LAI_{upper} above

148   2.5 m^2 m^{-2}. Where total tree LAI (LAI_{upper}) is between 0.8 and 2.5 m^2 m^{-2}, dominant vegetation type is

149   savanna, and LAI_{upper} values smaller than 0.8 m^2 m^{-2} characterize a grassland vegetation type.

150   We assume that the vegetation types Tropical Evergreen Forest and the Tropical Deciduous Forest

151   in INLAND represents the Amazon rainforest, while Savanna and Grasslands represent the Cerrado.

152   Savanna would be equivalent to the Cerrado physiognomies *Cerradão* and *Cerrado sensu strictu*, while

153   Grasslands would be equivalent to the physiognomies *Campo sujo* and *Campo Limpo* (*sensu* Ribeiro and

154   Walter, 2008).

155   The soil chemical properties are represented by the carbon, nitrogen and phosphorus. The carbon

156   cycle is simulated through vegetation, litter and soil organic matter, where the biogeochemical module is

157   similar to the CENTURY model (Parton et al., 1993; Verberne et al., 1990). The amount of C existing in

158 the first meter of soil is divided into different compartments characterized by their residence time, which

159 can vary in an interval of hours for microbial AGB and organic matter to several years for lignin. The

160 model considers only the soil N transformations and carbon decomposition, but the N cycle is not fully

161 simulated and N does not influence the vegetation productivity, i.e., there is a fixed C:N ratio. The P cycle

162 also is not fully implemented, instead the P-limitation is spatially parameterized through the linear relation

163 developed by Castanho et al. (2013) to limit the gross primary productivity. A map of total P available in

164 the soil (P_{total}) is used by the model to estimate the maximum capacity of carboxylation by the Rubisco

165 enzyme (V_{max}) for each grid using Equation (1) :.

166 $$V_{max} = 0.1013\, P_{total} + 30.037 \tag{1}$$

167 where V_{max} and P_{total} are given in $\mu molCO_2\ m^{-2}\ s^{-1}$ and $mg\ kg^{-1}$, respectively. This equation has been based

168 on data for tropical evergreen and deciduous trees, and is applied only to these two PFTs, the other PFTs

169 are unaffected.

170   INLAND also contains a spatial fire module, based on the Canadian Terrestrial Ecosystem Model

171 CTEM (Arora and Boer, 2005). In this module, three aspects of the fire triangle are considered – the

172 availability of fuel to burn, the flammability of vegetation, and the presence of an ignition source. Each

173 is represented daily by an independently calculated probability and the product of the three is the

174 probability of fire occurrence, calculated daily. Availability of fuel to burn depends on biomass,

175 flammability depends on soil moisture and ignition depends on a random lightning occurrence and a

176 constant anthropogenic ignition probability. The daily fire occurrence probability is equal to the daily

177 AGB burned fraction. The AGB burned fraction is accumulated throughout the year and its ratio is applied

178 at the end of each year to the grid cell area, reducing the leaf, wood and root biomass pools.

2.3 Observed data

2.3.1 Phosphorus databases

We used two P databases to estimate V_{max} (Equation 1): one regional (referred to as PR) and one global database referred to as PG). In addition, a control P map (PC) represents the unlimited nutrient availability case, equivalent to a V_{max} of 65 $\mu molCO_2$ m^{-2} s^{-1}, or 350 mg P kg^{-1} soil, according to Equation 1.

The PR database was developed from total P in the soil for the Amazon basin published by Quesada et al. (2011) plus 54 additional available P samples (P extracted via Mehlich-1 extractor, $P_{mehlich-1}$) (Figure 2a). We used the $P_{mehlich-1}$ and clay contents measured in a forest-savanna transition region in Brazil (Mato Grosso state) to estimate P_{total} and expand the coverage area of the P data (Section S1). These 54 samples were gridded to a $1° \times 1°$ grid to be compatible with the spatial resolution used by INLAND, resulting in 12 additional pixels with observed total P content (Figure 2a). For pixels without observed P_{total}, the P_{total} was assumed to be 350 mg P kg^{-1} soil, similarly to the PC conditions.

A global dataset of P_{total} (Figure 2b) was also used to estimate V_{max}. This global data set is part of a database containing six global maps of the different forms of P in the soil (Yang et al., 2013). The P_{total} was estimated from lithologic maps, distribution of soil development stages, fraction of the remaining source material for different stages of weathering using chronosequence studies (29 studies), and P distribution in different forms for each soil type based on the analysis of Hedley fractionation (Yang and Post, 2011), which are part of a worldwide collection of soil profile data. The uncertainties and limitations associated with this database are restricted to the Hedley fractionation data used, which are 17% for low weathered soils, 65% for intermediate soils and 68% for highly weathered soils (Yang et al., 2013).

2.3.2   Above-Ground Biomass (AGB) database

The AGB database used was created by Nogueira et al. (2015) and considered undisturbed (pre-deforestation) vegetation existing in the Brazilian Amazonia. This database was compiled from a vegetation map at a scale of 1:250000 (IBGE, 1992) and AGB averages from 41 published studies that had conducted direct sampling in either forest (2317 plots) or non-forest or contact zones (1830 plots). We bi-linearly interpolated the AGB (dry weight) for each transect considering $1° \times 1°$ to ensure compatibility of the observed and simulated data.

Five longitudinal transects (Figure 1) were individually used to characterize AGB in the Amazon-Cerrado border (Figures 3a and 3b). In T1, T2, T3 and T4, the higher AGB values in the west and lower values in the east are consistent with the transition from a dense and woody vegetation (the Amazon forest) towards a sparse vegetation with lower AGB (the Cerrado). However, T1 shows a more gradual reduction of AGB along the west to east gradient, while in T2, T3 and T4 where the transition is more abrupt. In T5 no west-east gradient is present with high AGB heterogeneity and predominant low AGB across the transect (Figure 3b).

2.4   Simulations

The model was forced with the prescribed climate data based on the Climate Research Unit (CRU) database (Harris et al., 2014). Two climate boundary conditions were used: the first is referred to as the monthly climatological average (CA) that represents the average climate for the period 1961-1990. The second climate boundary condition is the historical dataset, for the continuous period between 1948 and 2008, thus considering interannual climate variability (CV). For both boundary conditions, the variables

221 used are rainfall, solar radiation, wind velocity and maximum and minimum temperatures. The CRU

222 database is developed from observations at meteorological stations across the world's land areas and has

223 been widely used by the scientific community in case studies to evaluate El Niño–Southern Oscillation

224 (ENSO) effects and and other modes of interannual climate variability (Foley et al., 2002; Marengo, 2004;

225 Wang et al., 2014), because these data preserve the spatial mean of the rainfall data, although they do not

226 provide adequate representation of the precipitation variance (Beguería et al., 2016). The dataset has a 1-

227 degree spatial resolution and a monthly time resolution.

228 Soil texture data is based on the IGBP-DIS global soil (Global Soil Data Task 2000) (Hansen and

229 Reed, 2000). In the CV group of runs, the model was spin-up by cycling the 1948-2008 climate data (61-

230 year) seven times, totaling 427 years. In the CA group of runs, the annual mean climate data was cycled

231 427 times. In both cases, CO_2 varied from 278 to 380 ppmv, according to observations in the period,

232 updated annually. In both cases, only the model results of the last 10 years were used to analyze the

233 results.

234 The experiment design is a factorial combination of the climate scenarios (CA, monthly

235 climatological average, 1961-1990; CV, monthly climate time series, 1948-2008), the nutrient limitation

236 on V_{max} (PC, no P limitation ($V_{max} = 65$ $\mu molCO_2$ m^{-2} s^{-1}); PR, regional P limitation; PG, global P

237 limitation) and the occurrence of fire (F) or not (Table 1). The 12 combinations in Table 1 allow the

238 evaluation of individual and combined effects of climate, soil chemistry, and the incidence of fire on the

239 variables: Net Primary Production (NPP), tree AGB, and LAI of the upper and lower canopies (LAI_{upper},

240 LAI_{lower}).

241   We consider that the subtraction between the simulations (CV+PC) and (CA+PC) represents the

242   isolated effect of inter-annual climate variability without P limitations. The same logic is applied to isolate

243   other factors such as fire and P in different climate scenarios. For example, the fire effect under average

244   climate without P limitation case is calculated by the difference between CA+PC+F and CA+PC.

245   Similarly, the isolated effect of fire under a climate with inter-annual variability scenario without

246   influence of P limitation is calculated by the difference between CV+PC+F and CV+PC. The different

247   combinations of climate scenarios with and without fire effects and with and without P limitations are

248   described in Table 2.

249   **2.5   Statistical analysis and determination of the best model configuration**

250   The statistical analysis is divided in four parts. First, we present maps of the isolated effects for

251   all simulated area calculated as the average of last ten years of simulated spatial patterns. The statistical

252   significance of the isolated effects on NPP, LAI and AGB are determined using the t-test with $p < 0.05$.

253   The results are tested in each pixel, for all the simulated domain ($n = 10$).

254   Second, we present an analysis of variance using the one-way ANOVA and the Tukey-Kramer

255   test in the transition zone. We consider all 31 pixels which fall in transects T1 to T5 (n_{pixels}). The results

256   presented are based on the set of last 10 years of simulation (1999-2008, n_{years}) for the 12 combinations

257   ($n_{simulation}$) in Table 1. Moreover, we grouped treatments according to climate regardless of P limitation,

258   presence or absence of fire, where all sets with CV vs CA are tested (Group 1, n=1860, (n_{pixel} x n_{year} x

259   ($n_{simulation}$/2)). Similarly, in Group 2 we tested if PC, PR or PG were significantly different from each other

260   regardless the F or climate used (Group 2, n=1240, (n_{pixel} x n_{year} x ($n_{simulation}$/3)). In Group 3 we tested if

261   fire introduced a significant effect regardless of climate and P limitation (Group 3, n=1860, (n_{pixel} x n_{year}

262 x ($n_{simulation}$/2)). Finally, all treatments were tested to each simulation assessing their individual effects on

263 NPP, LAI and AGB (n_{pixel} x n_{year} = 310).

264   Third, a correlation coefficient between the simulated and observed values for AGB was

265 calculated for each transect. The simulated variables are averaged for the last 10 years of simulations

266 (1999 - 2008) and compared to AGB from Nogueira et al. (2015) within a grid cell.

267   Finally, we evaluate INLAND's ability to assign the dominant vegetation type by analyzing 10

268 years of probability of occurrence. If the dominant vegetation type (evergreen tropical forest, or deciduous

269 forest for the Amazon rainforest, and savanna or grasslands for Cerrado) in a pixel is the same in more

270 than 90% of the simulated years (9 out of 10), then the simulated vegetation type is defined as "very

271 robust" for that pixel; if it occurs in 70 – 90% of the simulated years, the simulated result is considered to

272 be "robust". If the dominant vegetation occurred in less than 70% of simulated years, the pixel is

273 considered "transitional" vegetation.

274 **3   Results**

275 **3.1   Influence of climate, fire and phosphorus in the Amazon-Cerrado transition region**

276 **3.1.1   Spatial patterns**

277   Overall, the inclusion of inter-annual climate variability (CV) resulted in a decrease in the

278 simulated average tree biomass (TB) by 3.8% in the entire Brazilian Amazonia, and by 8.7% in the entire

279 Cerrado in comparison to average climate (CA), values obtained by difference CV+PC – CA+PC (Figure

280 4a). The spatial differences between CV and CA for TB simulations are statistically significant and range

281 from -3 kg-C m^{-2} to +2 kg-C m^{-2}. The state of Pará, with higher influence of the El Niño phenomenon,

282 experienced the highest decrease in TB in the CV simulation. In the state of Roraima, on the other hand,

283 there was an increase of about 2 kg-C m^{-2} in TB when CV was considered. Bolivia and southwest of Mato

284 Grosso state also presented, in some grids points, a significant increase in AGB higher than 2 kg-C m^{-2}.

285   On average, P acts as a limiting factor in the simulated TB, decreasing by 13% in regional P (PR)

286 simulation and 15% in global P (PG) simulation. In PR, TB decreased mainly in the southeastern

287 Amazonia (between Pará and northeastern Mato Grosso states) and northwestern Amazonas state (Figure

288 4b). In PG, the largest TB decline occurred in central Amazonia, northeastern Pará and northeastern Mato

289 Grosso (Figure 4c). In Cerrado, on the other hand, TB declined by 2% for PR and 9% for PG with respect

290 to the control simulation. In PR, the few pixels in the Cerrado that have P limitation showed a significant

291 decrease in TB (Figure 4b), while in PG the TB reduction was statistically significant for most of the

292 Cerrado domain, except in southern Tocantins state (Figure 4c).

293   The tree biomass reduction due to fire events is much higher in magnitude more than due to P

294 limitation or inter-annual climate variability (Figure 4d). The small or null fire effect in the Central

295 Amazon rainforest is related the greater water availability on the Amazonia, which makes the forest

296 naturally not flammable as well as a gradient towards seasonally dryer climate increases the intensity and

297 magnitude of fire effects towards the Cerrado (Figure 4d). The fire effect on TB over the Amazon domain

298 was 21-24% of the P limitation effect (range for PR and PG cases), while the fire effect on TB over the

299 Cerrado was more than 250% of the P limitation effects in CV simulations, which is due to quick growth

300 of grasses after fire occurrence in the latter.

3.1.2 Influence of climate, fire and phosphorus in the transects

Results of the ANOVAs and Tukey-Kramer test indicate that the inclusion of CV, limitation by P (PR and PG) and fire in INLAND led to significantly different averages of NPP, LAI and AGB in the transition zones. This influence of climate, P and fire are shown separately in Tables 3 to Table 5 and combined in Table 6.

The effects of climate and P on productivity show that CV reduces the NPP from 0.68 kg-C m^{-2} yr^{-1} to 0.64 kg-C m^{-2} yr^{-1} (Table 3) and the P effect results in NPP decline from 0.71 kg-C m^{-2} yr^{-1} to 0.64 kg-C m^{-2} yr^{-1} (both PR and PG) (Table 4). The fire effect, moreover, has a positive effect on NPP from 0.66 kg-C m^{-2} yr^{-1} when fire is off to 0.67 kg-C m^{-2} yr^{-1} when fires is on. This difference, albeit low, is statistically significant (Table 5).

In addition CV and P limitation reduce the LAI$_{total}$ in the canopy (Table 3 and Table 4), increasing three times LAI$_{lower}$ and decreasing LAI$_{upper}$ (Table 5). The magnitude of fire effect on AGB (46.7%, Table 5) is greater in relation to the CV (5%, Table 3) and P (14%, Table 4) limitation effects.

Even though CV effects on NPP and AGB for each simulation is not statistically significant, the effects of fire and P limitation (regardless of phosphorus map) are. Fire effects are significant only for structural variables as AGB, LAI$_{total}$, LAI$_{upper}$ and LAI$_{lower}$. It presents an increase of LAI total of 1.52 m^2 m^{-2} in CV+PG+F in relation to CV+PG, and of 1.32 m^2 m^{-2} in CV+PR+F in relation to CV+PR (Table 6).

3.1.3 West-East patterns of AGB in the Amazon-Cerrado transition

The model used in this study simulates > 80% of the observed AGB variability in all treatments along the transition area except in T5 (Table 7). It shows that the model is able to capture AGB variability

along the transition area, which is relevant when compared to studies that simulate 50% of the observed AGB variability (Senna et al., 2009; Castanho et al., 2013).

It is not possible to identify a treatment that best represents AGB in all transects (Table 7). A combined analysis of Table 7 and Figure 5 indicates a general agreement that observed AGB decreases from W to E in T1 to T4, and this is well captured by several configurations of the model, with specific differences among them. Overall, CA and PC configurations, being the least disturbed treatments, yield higher AGB, while the introduction of CV, PG and F reduce the AGB. However, the simulated results may be above or below the observed ones, which suggests that additional local factors are not included in the model.

The curves of AGB (Figure 5) show the impact of CV, PG and F along the W-E transition. PG has a high influence on the transition, decreasing the ABG especially in the western part of the transects, where the Amazon vegetation is predominant. This feature is particularly simulated in T3 and T4, where PG decrease the AGB by 2 kg-C m^{-2} in the west pixels of these transects (Figure 5). In T1, T2 and T5, AGB decline is also higher with P limitation when compared to the curves limited only by CV. However, in T1 model simulations tend to underestimate the highest and the lowest AGB extremes, and the absolute values were always underestimated, despite the improvement in correlation with the inclusion of the fire component (Table 7).

In T2, T3 and T4, however, fire changes the simulated AGB, making it closer to the observed AGB in the eastern pixels of the Cerrado domain (Figure 5). In T5 these relations are similar, with climate presenting less influence on AGB decrease than P, and fire appears mainly as an AGB reduction factor.

3.2   Simulated composition of vegetation

Most of the pixels in CA show very robust simulations, with more than 90% of the same vegetation cover in the simulated last 10 years (Figure 6a-c and 6g-i). A larger number of pixels with transitional vegetation were simulated in CV (Figure 6d-f and and 6j-l). An even higher variability in CV compared to CA simulations was observed when we added the effects of P limitation and fire (Figure 6a and 6j-l).

The vegetation composition in all P limitation scenarios for CA simulations resulted in robust simulations for nearly all pixels, except for the north of Cerrado domain (Figures 6a, 6b and 6c). The CA+PC and CA+PR simulations had the same vegetation composition, while CA+PG replaced the deciduous forest by evergreen forest in the central Cerrado region, around 8°S 46°W (Figures 6A, 6B and 6C). This behavior might be related to the higher P_{total} values in PG than PR and PC for the Cerrado region (Figure S1). Cerrado was better represented in CV+PC, CV+PR and CV+PG than in the same CA combinations (Figure 6). The occurrence of forested areas in central Cerrado decreased in CV combinations, these being replaced by the savanna or grassland vegetation class.

When the effect of fire was added to CA simulations, the model simulated an increase in the uncertainty on the vegetation cover classification in the Cerrado region. The effect of fire reduced the presence of deciduous forest in central Cerrado biome as well as in CA+PC, and the vegetation was replaced by evergreen forest in about 5 pixels with clay soils with large water retention capacity in CA+PC+F (Figures 6G, 6H, 6I). In this situation, where there is little water stress in the CA simulation, both evergreen and drought deciduous PFTs have each one very high LAI, and the PFT that dominates can be defined by minor effects. Fire, although active, is probably too small to be relevant in a non-stressed ecosystem. In CV simulations, however, fire effect results in the replacement of the deciduous

363 and perennial forest by savanna and grasses in all central Cerrado region (Figures 6J, 6K and 6L). These

364 results show the limitations of CA and the importance to consider the interannual climate variability on

365 simulations to improve the vegetation simulated.

366   For all combinations used, transitional forest areas in the northern and southwestern Cerrado

367 biome are not adequately represented. With >90% of concordance, INLAND assigns the existence of

368 tropical evergreen forest rather than deciduous forest in some pixels in the north of the transition, and the

369 existence of tropical evergreen forest rather than savanna in the southwest, indicating difficulty to

370 simulate transitional vegetation in these regions.

371 **4   Discussion**

372   The inclusion of CV, PR and PG and fire in INLAND showed significant influences on the

373 simulated vegetation structure and dynamics in the Amazon-Cerrado border (Figure 4 and Table 6),

374 suggesting that these factors play key role on vegetation structure in the forest-savanna border and can

375 improve the simulated representation of the current contact zone between these biomes. This is broadly

376 consistent with the literature that investigated causes of savanna existence in the real world (Hoffmann et

377 al., 2012; Dantas et al., 2013; Lehmann et al., 2014). In this study, the spatial analysis and the Tukey-

378 Kramer test (TK) show a difference in magnitude among these factors in vegetation, with fire occurrence

379 and P limitation being stronger than inter-annual climate variability along the transects (Figure 4).

380   The spatial analysis showed that CV declines AGB predominantly in eastern Amazonia (Figure

381 4a). Climate of this region is intensely affected by ENSO, which could reduce precipitation by 50%,

382 placing the vegetation under intense water stress (Botta and Foley, 2002; Foley et al. 2002; Marengo et

383 al., 2004; Andreoli et al., 2012; Hilker et al., 2014). This reduction in rainfall in dry years brings in direct

384   changes in carbon flux (NPP) and stocks in leaves and wood, leading to changes in vegetation structure.

385   In addition to inter-annual changes in the rainfall, inter-annual variability in other climate variables in CV

386   also affect AGB, as average, maximum and minimum temperature, as well as wind speed and specific

387   humidity, and influence photosynthesis on the model both directly (through Collatz and Farquhar

388   equations) and indirectly (e.g. through evapotranspiration). Our results showed significant differences for

389   most part of the biomes, except central Amazonia (Figure 4a), where CV and precipitation seasonality

390   have been pointed as secondary effects on vegetation (Restrepo-Coupe et al., 2013), since there is no

391   shortage of water availability during the dry season.

392   Along the Cerrado, lower water availability in some years in CV affects tree biomass, although

393   that vegetation is predominantly grassy-herbaceous. The AGB decline is significant for most part of the

394   simulated Cerrado domain (Figure 4a) and average values could represent half the amount of typical tree

395   biomass in this biome. This reduction in AGB reflects INLAND's ability to simulate similar Cerrado

396   conditions and expose the few trees to high water stress.

397   Throughout the transects, however, no significant difference was found for average AGB between

398   CV+PC and CA+PC by TK at p<0.05 (Table 6). On the other hand, when we analyzed the influence of

399   CV for the same pixels, but using all simulations (Table 3), regardless of P limitation and fire occurrences,

400   the results showed that the decrease in AGB by 0.38 kg-C m^{-2} (5.7%) is statistically significant along the

401   transition.

402   P limitation effect was statistically significant for PR and PG along all the Amazon domain and

403   the main differences between these simulations were the spatial patterns of tree AGB decrease (Figure 4b

404   and Figure 4c). We cannot affirm which of these databases is better because they are the results of

different methodologies and observations (Quesada et al., 2009; Yang et al., 2014). However, PG showed a higher AGB decrease in central Amazonia, northeastern Pará and northeastern Mato Grosso state, indicating that in these areas the P limitation is higher. This result does not corroborate the northwest-southeast AGB gradient found in the Amazon basin, which showed a higher productivity in the west where soils are more fertile than those found in the southeast (Aragão et al., 2009; Saatchi et al., 2007; Nunes et al., 2012; Lee et al., 2013). On the other hand, PR AGB agrees with the northwest-southeast gradient, presenting less limitation in the soils of central Amazonia with declines in AGB mainly in the southeastern part of the rainforest (between Pará and northeastern Mato Grosso states) (Figure 4b).

In Cerrado, P limitation also influenced vegetation (Figure 4c) and presented statistically significant differences when compared CV+PG – CV+PC. In this biome, as well as in the Amazon, tree abundance richness and diversity have been generally associated with increases of soil fertility (Long et al., 2012; Vourtilis et al., 2013), highlighting the importance of P in the composition and maintenance of vegetation, especially in transition areas.

Compared to the Amazon domain, the magnitude of effects of P limitation is lower in the Cerrado. However, few pixels in PR that have P limitation showed a significant decrease in arboreal AGB (Figure 4b), while in PG, we found reduction of AGB for most of the Cerrado domain, except only for the southern Tocantins state (Figure 4c). Despite the differences in spatial patterns, there was no statistically significant differences between PR and PG within the transects (Table 4 and Table 6).

The spatial difference between PG and PR showed that PG is lower than PR in the western Amazonia, and higher in northern Amazonia. Moreover, PG have low P values in south of the transition compared to PR, while in Cerrado domain P values ranged between 120 to 200 mg kg^{-1} (Figure S1).

426   Although the PR dataset includes every known P data collected in the region, these differences reinforce

427   the need to improve the data of P_{total} in the soils of the Amazon and Cerrado/Amazon transition domains.

428   Currently, P_{total} data in Cerrado is scarce, and make unfeasible to establish a proxy similar to Castanho et

429   al. (2013), which was specific for the Amazon.

430   In INLAND, the simple P-limitation parameterized through the linear relation Vmax and P_{total},

431   showed significant spatial differences in AGB simulated and an improvement in simulations, highlighting

432   the importance of P-limitation in modeling studies. For the most part, Dynamic Global Vegetation Models

433   (DGVMs) do not consider the complete phosphorus cycle (see exceptions in Goll et al., 2012 and Yang

434   et al., 2014), despite the importance of nutrient cycling for AGB maintenance and tropical vegetation

435   dynamics in dystrophic soils. For example, nutrient cycling in the Amazon/Cerrado transition is closely

436   related to the hyper-dynamic turnover of the AGB (Valadão et al. 2016), in which some key species might

437   also be crucial to the hyper-cycling of nutrients through which vegetation sustain the constant input of

438   nutrients, including large annual amounts of available P (Oliveira et al. 2017). In addition, there is

439   influence between weather and nutrients: a very intense rain can leach nutrients, such as nitrogen, as well

440   as strong winds can carry clay particles where numerous nutrients are adsorbed. However, in this work

441   the nutritional conditions are prescribed and fixed.

442   The fire occurrence is an important factor controlling the AGB dynamics in the Cerrado or in the

443   transition vegetation (Hoffman et al.,2003; Hoffman et al., 2012; Silvério et al., 2013; Couto-Santos

444   al., 2014; Balch et al., 2015), which this study clearly replicates, showing statistically significant

445   influences when compared to control simulations (Figure 4d and Table 5). In the transition, the fire effect

446   may reduce average AGB by 50% (Table 5), which under climate change or deforestation conditions may

447 lead to an even stronger change in the vegetation structure and dynamics. In INLAND, the fire disturbance

448 reduces the biomass of all pools and PFT's by the same fraction inside each pixel at the end of every year.

449 Thus, upper and lower LAI are decreased, according to the fire probability, triggering competition

450 between both canopies for light, and increasing the photosynthesis rates and stocks of carbon in leaves,

451 stems and roots pools in the lower canopy. The carbon allocation and mortality rates in INLAND are

452 fixed parameters for each PFT and are not modified after fire occurrence. Thus, during recovery from a

453 fire, the vegetation dynamics follows the model standard procedure.

454 The dynamics between the upper and lower canopies and the changes in canopy structure after

455 fire occurrence are exclusively due to the canopy opening and consequently more penetration of

456 photosynthetic radiation into the lower canopy. This competition implies in significant increase on the

457 lower canopy resulting in increment of LAI_{lower} (Table 5).

458 The model does not include fire characteristics such as velocity, intensity and duration of the

459 burning (Hoffman et al., 2003; Rezende et al., 2005; Elias et al., 2013; Reis et al., 2015) or the

460 representation of some tree morphological adaptation that confers to Cerrado species resilience to fire

461 occurrence, such as bark thickness. Thus, trees and grasses throughout the Amazon-Cerrado border are

462 equally exposed to the same fire intensity inside the grid cell, without fire resistance differences.

463 However, despite the limitations in the representation of resilience characteristics and morphological

464 attributes of fire resistance, our results show that simulated biomass is more close to observed biomass in

465 Cerrado areas when the fire module is activated (Figure 5). An improvement in distribution of biomes

466 along the simulated transition area is also observed (Figure 6g-i), highlighting fire as an essential factor

467 to represent the Amazonia-Cerrado border.

468   This study shows an improvement in the correlations between simulated and observed AGB when

469   compared to previous modeling studies, regardless of treatment, with correlation coefficients usually

470   above 0.80 for the transects, except for T5, for which the correlation coefficient value is usually below

471   0.5 (Table 7). Senna et al. (2009) found 0.20 as maximum correlation coefficient between simulated and

472   observed ABG while Castanho et al. (2013) showed 0.80 for Amazonia domain. From Figure 5, it is clear

473   that CV, F and P limitation in the transition zone reduce the AGB, causing the simulated data to approach

474   the observed data. However, the inclusion of these effects is still insufficient to represent the correct

475   distribution of the vegetation types throughout the Amazon-Cerrado border (Figure 6L). In our

476   interpretation, this means that other important factors are still missing from the simulation, especially in

477   T5, where soils are rocky and shallow. A better spatial representation of soil physical properties, including

478   shallow rocky soils, as well as spatially varying physiological parameterizations of the vegetation such as

479   carbon allocation, deciduousness of vegetation, residence time, are probably needed to improve the

480   simulations, in particular in the northern and southern extremes of the border (T1 and T5).

481   In addition, literature shows that in the transition area, soils are very different than Amazon soils,

482   and that essential proprieties for modeling are peculiar (Silva et al., 2006; Vourlitis et al., 2013; Dias et

483   al. 2015). For example, Dias et al. (2015) recently showed that the pedological functions normally used

484   by DGVMs may underestimate the saturated hydraulic conductivity (K_s) by >99%, transforming a well-

485   drained   soil   with $K_s = 1.5.10^{-4}$ m.s^{-1} (540   mm.h^{-1})   in   reality   into   an   impervious   brick   with

486    $K_s = 3.3.10^{-7}$ m.s^{-1} (1.2 mm.h^{-1}) in the model.

487   For all transects, the AGB curves have similar patterns (Figure 5); the smaller difference is

488   observed between CA+PC and CV+PG curves, while the larger difference is when fire is present. The

489   effect of P limitation appears as an effect of intermediate magnitude, reducing the AGB by more than the

490   effect of inter-annual climate variability. In the east, it is observed that there is little or no difference

491   among AGB simulated by CA+PC, CV+PC and CV+PG, revealing that inter-annual climate variability

492   and P have smaller influence in the AGB. However, in the east of T2, T3 and T4, fire is the factor that

493   adjusts the simulated to the observed data (Figure 5), differently than the grid points in the West, where

494   CV+PG is a better proxy between observed and simulated data.

495   Such conditions are interesting because they reflect the different mechanisms that regulate the

496   structure of these ecosystems and probably the phytophysiognomies distribution. For example, P

497   limitation seems to be the factor that improves simulated AGB in regions where the predominant

498   vegetation type is the tropical rainforest. Fire, on the other hand, improves the AGB in grid points where

499   the Cerrado occurs. Moreover, important factors such as productivity partitioning into leaves, roots and

500   wood carbon pools are assumed to be fixed in space and time within a given PFT, neglecting the natural

501   capacity of transitional forests to adapt itself and to adjust their metabolism to local environmental

502   conditions (Senna et al., 2009). In years of severe drought, or under frequent fire occurrence, transitional

503   forests could prioritize the stock of carbon in fine roots instead of the basal or leaf increment to maximize

504   access to available water, make hydraulic redistribution of soil moisture to maintain the greenness and

505   photosynthesis rates, or increase the capacity to resprout after fire occurrence (Hoffman et al., 2003;

506   Brando et al., 2008). Brando et al. (2008) found changes in carbon allocation after an artificial drought in

507   eastern Amazonia, with wood production reduced by 13-60%, and associated increase in root production.

508   Although in INLAND low soil moisture can reduce the photosynthetic rates, carbon allocation rates are

509   fixed (Figure 5a).

T2, T3 and T4, located in the central part of the Amazon-Cerrado transition, showed the highest average correlations between observed and simulated data (Table 7). For these transects, INLAND seems to be able to capture the high variability of AGB gradient.

At T5, located at the south of the transition, the average correlations were low for all treatments, indicating that INLAND has difficulty to represent the AGB gradient there (Table 7). However, it captures the lower AGB as compared to the northern ones. In this region, the vegetation is characterized by a wide diversity of physiognomies, which varies with other preponderant factors, such as lithology, soil depth, topography and fertility. The observed data also showed high AGB variability, indicating that there are changes in the vegetation structure, featuring medium-sized and small vegetation types on different soil types. In INLAND, however, features such as lithology and water-table depth are not considered due to the complexity of its representation on the large scale, limiting the representation of a heterogeneous environment throughout the transition.

Patterns of vegetation distribution along the Amazon-Cerrado border exist are influenced not only by inter-annual climate variability, P limitation, and fire, but also by the ecophysiological parameters. Additional field experiments are needed to understand the relationship between currently fixed parameters (such as carbon allocation, residence time, and deciduousness, among others) to the environmental conditions and soil proprieties.

Another point to discuss is that the model simulates, in a few pixels in southeastern Cerrado, very robust simulations of the presence of savanna and grassland even in the absence of fire (Figure 6A-F and 6a-f). This is, in our view, a result of the intense water and heat stress in this region. In the Brazilian Cerrado, the high temperatures (> 35 °C) combined to the dry season duration (as long as 6 months with

531   little or no rain) exposes the vegetation to a severely stressed situation, so that a low biomass, low LAI

532   vegetation may exist without the need of a frequent disturbance.

533

534   **5   Conclusions**

535   This is the first study that uses modeling to assess the influence of inter-annual climate variability,

536   fire occurrence and phosphorus limitation to represent the Amazon-Cerrado border. This study shows

537   that, although the model forced by a climatological database is able to simulate basic characteristics of

538   the Amazon-Cerrado transition, the addition of factors such as inter-annual climate variability,

539   phosphorus limitation and fire gradually improves simulated vegetation types. These effects are not

540   homogeneous along the latitudinal/longitudinal gradient, which makes the adequate simulation of

541   biomass challenging in some places along the transition. Based on the F-statistic in Tables 3, 4 and 5, this

542   work shows that fire is in the main determinant factor of the changes in vegetation structure (LAI, AGB)

543   along the transition. The nutrient limitation is second in magnitude, stronger than the effect of inter-annual

544   climate variability.

545   Overall, although INLAND typically simulates more than 80% of the variability of biomass in the

546   transition zone, in many places the biomass is clearly not well simulated. Situations for clearly wet or

547   markedly dry climate conditions were well simulated, but the simulations are generally poor for

548   transitional areas where the environment selected physiognomies that have an intermediate behavior, as

549   is the case of the transitional forests in northern Tocantins and Mato Grosso.

550   There is evidence that the inclusion of spatially explicit parameters such as woody biomass

551   residence time, maximum carboxylation capacity (V_{max}), and NPP allocation to wood may improve

Amazon rainforest AGB simulation by DGVMs (Castanho et al., 2013). However, in the transition, the lack of field parameters measured limits the inclusion of the variability of these biophysical parameters in DGVMs. Additional field work and compilation of existing ones are necessary to obtain physiological and structural parameters through the Amazon-Cerrado border to establish numerical relationships between soil, climate and vegetation. With the help of these data, dynamic vegetation models will be able to improve simulation of current patterns and future changes in vegetation considering climate change scenarios. In addition, it is also needed to include not only the spatial variability, but also temporal variability in physiological parameters of vegetation, allowing a more realistic simulation of the soil-climate-vegetation relationship. Finally, our results reinforce the importance and need of the DGVMs to incorporate the nutrient limitation and fire occurrence to simulate the Amazon-Cerrado border position.

6   Acknowledgements

We gratefully thank the Brazilian agencies FAPEMIG and CAPES for their financial support. Atul K Jain is funded by the U.S. National Science Foundation (NSF-AGS- 12-43071).

7   References

Andreoli, R. V., Ferreira de Souza, R. A., Kayano, M. T. and Candido, L. A.: Seasonal anomalous rainfall in the central and eastern Amazon and associated anomalous oceanic and atmospheric patterns, Int. J. Climatol., 32(8), 1193–1205, doi:10.1002/joc.2345, 2012.

Aragão, L. E. O. C., Malhi, Y., Metcalfe, D. B., Silva-Espejo, J. E., Jiménez, E., Navarrete, D., Almeida, S., Costa, A. C. L., Salinas, N., Phillips, O. L., Anderson, L. O., Baker, T. R., Goncalvez, P. H., Huamán-Ovalle, J., Mamani-Solórzano, M., Meir, P., Monteagudo, A., Peñuela, M. C., Prieto, A.,

573 Quesada, C. A., Rozas-Dávila, A., Rudas, A., Silva Junior, J. A. and Vásquez, R.: Above- and below-

574 ground net primary productivity across ten Amazonian forests on contrasting soils, Biogeosciences, 6,

575 2441–2488, doi:10.5194/bgd-6-2441-2009, 2009.

576 Arora, V. K. and Boer, G. J.: Fire as an interactive component of dynamic vegetation models, J.

577 Geophys. Res, 110, doi:10.1029/2005JG000042, 2005

578 Balch, J. K., Brando, P. M., Nepstad, D. C., Coe, M. T., Silvério, D., Massad, T. J., Davidson, E.

579 A., Lefebvre, P., Oliveira-Santos, C., Rocha, W., Cury, R. T. S., Parsons, A. and Carvalho, K. S.: The

580 Susceptibility of Southeastern Amazon Forests to Fire: Insights from a Large-Scale Burn Experiment,

581 Bioscience, 65(9), 893–905, doi:10.1093/biosci/biv106, 2015.

582 Beguería, S., Vicente-Serrano, S. M., Tomás-Burguera, M. and Maneta, M.: Bias in the variance

583 of gridded data sets leads to misleading conclusions about changes in climate variability. Int. J. Climatol.,

584 36: 3413–3422. doi:10.1002/joc.4561, 2016.

585 Betts, R. A., Cox, P. M., Collins, M., Harris, P. P., Huntingford, C. and Jones, C. D.: The role of

586 ecosystem-atmosphere interactions in simulated Amazonian precipitation decrease and forest dieback

587 under global climate warming, Theor. Appl. Climatol., 78, 157–175, doi:10.1007/s00704-004-0050-y,

588 2004.

589 Bonan, G. B.: Forests and climate change: forcings, feedbacks, and the climate benefits of forests,

590 Science, 320(5882), 1444–1449, doi:10.1126/science.1155121, 2008.

591 Bond, W. J., Woodward, F. I. and Midgley, G. F.: The global distribution of ecosystems in a world

592 without fire, New Phytol., 165(2), 525–538, doi:10.1111/j.1469-8137.2004.01252.x, 2005.

593   Botta, A. and Foley, J. A.: Effects of climate variability and disturbances on the Amazonian

594   terrestrial ecosystems dynamics, Global Biogeochem. Cycles, 16(4), doi:10.1029/2000GB001338, 2002.

595   Brando, P. M., Nepstad, D. C., Davidson, E. A., Trumbore, S. E., Ray, D. and Camargo, P.:

596   Drought effects on litterfall, wood production and belowground carbon cycling in an Amazon forest:

597   results of a throughfall reduction experiment, Philos. Trans. R. Soc. Lond. B. Biol. Sci., 363(1498), 1839–

598   48, doi:10.1098/rstb.2007.0031, 2008.

599   Castanho, A. D. A., Coe, M. T., Costa, M. H., Malhi, Y., Galbraith, D. and Quesada, C. A.:

600   Improving simulated Amazon forest AGB and productivity by including spatial variation in biophysical

601   parameters, Biogeosciences, 10(4), 2255–2272, doi:10.5194/bg-10-2255-2013, 2013.

602   Couto-Santos, F. R., Luizão, F. J. and Carneiro Filho, A.: The influence of the conservation status

603   and changes in the rainfall regime on forest-savanna mosaic dynamics in Northern Brazilian Amazonia,

604   Acta Amaz., 44(2), 197–206, 2014.

605   Cox, P. M., Betts, R. A., Jones, C. D., Spall, S. A. and Totterdell, I. J.: Acceleration of global

606   warming due to carbon-cycle feedbacks in a coupled climate model, Nature, 408(November), 184–187,

607   doi:10.1038/35041539, 2000.

608   Cox, P. M., Betts, R. A., Collins, M., Harris, P. P., Huntingford, C. and Jones, C. D.: Amazonian

609   forest dieback under climate-carbon cycle projections for the 21st century, Theor. Appl. Climatol., 78,

610   137–156, doi:10.1007/s00704-004-0049-4, 2004.

611   Dajoz, R.: Princípios de ecologia, 7º edição, Artmed, Porto Alegre, RS, Brazil 519pp, 2005.

612   Dantas, V. L., Batalha, M. A. and Pausas, J. G.: Fire drives functional thresholds on the savanna-

613   forest transition, Ecology, 94(11), 2454–2463, doi:10.1890/12-1629.1, 2013.

614   Davidson, E. A., Carvalho, C. J.R., Vieira, I. C. G., Figueiredo, R. D. O., Moutinho, P., Ishida,

615   F.Y., Santos, M. T.P., Guerrero, J.B., Kalif, K. and Sabá, R.T.: Nitrogen and Phosphorus Limitation of

616   Biomass Growth in a Tropical Secondary Forest, Ecol. Appl., 14(4), 150–163, doi:10.1890/01-6006,

617   2004.

618   Dias, L. C. P., Macedo, M. N., Costa, M. H., Coe, M. T. and Neill, C.: Effects of land cover change

619   on evapotranspiration and streamflow of small catchments in the Upper Xingu River Basin, Central

620   Brazil, J. Hydrol. Reg. Stud., 4, 108–122, doi:10.1016/j.ejrh.2015.05.010, 2015.

621   Elias, F., Marimon, B. S., Matias, S. R. A., Forsthofer, M., Morandi, P. S. and Marimon-junior,

622   B. H.: Dinâmica da distribuição espacial de populações arbóreas, ao longo de uma década, em cerradão

623   na transição Cerrado-Amazônia, Mato Grosso, Biota Amaz., 3, 1–14, 2013.

624   Favier, C., Chave, J., Fabing, A., Schwartz, D. and Dubois, M. A.: Modelling forest-savanna

625   mosaic dynamics in man-influenced environments: Effects of fire, climate and soil heterogeneity, Ecol.

626   Modell., 171, 85–102, doi:10.1016/j.ecolmodel.2003.07.003, 2004.

627   Foley, J. A., Prentice, I. C., Ramankutty, N., Levis, S., Pollard, D., Sitch, S. and Haxeltine, A.: An

628   integrated biosphere model of land surface processes, terrestrial carbon balance, and vegetation dynamics,

629   Global Biogeochem. Cycles, 10, 603, doi:10.1029/96GB02692, 1996.

630   Foley, J. A., Botta,A., Coe, M. T. and Costa, M. H.: El Niño–Southern oscillation and the

631   climate, ecosystems and rivers of Amazonia, Global Biogeochem. Cycles, 16(4), 1132,

632   doi:10.1029/2002GB001872, 2002.

633   Goedert, W: Solos do Cerrado: Tecnologias e Estratégias de Manejo, Empresa Brasileira de

634   Pesquisa Agropecuária (EMBRAPA), Brasília, DF, Brasil. 422pp., 1986.

635   Goll, D. S., V. Brovkin, B. R. Parida, C. H. Reick, J. Kattge, P. B. Reich, P. M. Van Bodegom,

636   and Ü. Niinemets.: Nutrient limitation reduces land carbon uptake in simulations with a model of

637   combined carbon, nitrogen and phosphorus cycling, Biogeosciences, 9(C), 3547–3569, doi:10.5194/bg-

638   9-3547-2012,2012.

639   Hansen, M. C. and Reed, B.: A comparison of the IGBP DISCover and University of Maryland

640   1km global land cover products, Int. J. Remote Sens., 21, 1365–1373, doi:10.1080/014311600210218,

641   2000.

642   Harris, I., Jones, P. D., Osborn, T. J. and Lister, D. H.: Updated high-resolution grids of monthly

643   climatic observations - the CRU TS3.10 Dataset, Int. J. Climatol., 34(3), 623–642, doi:10.1002/joc.3711,

644   2014.

645   Hilker, T., Lyapustin, A. I., Tucker, C. J., Hall, F. G., Myneni, R. B., Wang, Y., Bi, J., Mendes de

646   Moura, Y. and Sellers, P. J.: Vegetation dynamics and rainfall sensitivity of the Amazon., Proc. Natl.

647   Acad. Sci. U. S. A., 111(45), 16041–6, doi:10.1073/pnas.1404870111, 2014.

648   Hirota, M., Nobre, C., Oyama, M. D. and Bustamante, M. M. C.: The climatic sensitivity of the

649   forest, savanna and forest-savanna transition in tropical South America, New Phytol., 187, 707–719,

650   doi:10.1111/j.1469-8137.2010.03352.x, 2010.

651   Hoffmann, W. A., B. Orthen, and P. K. V. Nascimento.: Comparative fire ecology of tropical

652   savanna and forest trees, Functional Ecology, 17:720–726, 2003.

653   Hoffmann, W.A., Adasme, R., Haridasan, M., Carvalho, M., Geiger, E.L., Pereira, M.A.B.,

654   Gotsch, S.G., and Franco, A.C.:Tree topkill, not mortality, governs the dynamics of alternate stable states

655   at savanna-forest boundaries under frequent fire in central Brazil, Ecology, 90, 1326–1337, 2009.

656 Hoffmann, W. A., Geiger, E. L., Gotsch, S. G., Rossatto, D. R., Silva, L. C. R., Lau, O. L.,

657 Haridasan, M. and Franco, A. C.: Ecological thresholds at the savanna-forest boundary: How plant traits,

658 resources and fire govern the distribution of tropical biomes, Ecol. Lett., 15, 759–768,

659 doi:10.1111/j.1461-0248.2012.01789.x, 2012.

660 House, J. I., Archer, S., Breshears, D. D. and Scholes, R. J.: Conundrums in mixed woody-

661 herbaceous plant systems, J. Biogeogr., 30, 1763–1777, doi:10.1046/j.1365-2699.2003.00873.x, 2003.

662 IBGE.: Manual Técnico da Vegetação Brasileira (Manuais Técnicos em Geociências n. 1),

663 Fundação Instituto Brasileiro de Geografia e Estatística (IBGE), Rio de Janeiro, RJ, Brasil. 92pp., 1992.

664 IBGE.: Mapa da Vegetação do Brasil, Fundação Instituto Brasileiro de Geografia e Estatística

665 (IBGE), Rio de Janeiro, RJ, Brazil, Map, 2004.

666 Klink, C. A. and Machado, R. B.: Conservation of the Brazilian Cerrado, Conserv. Biol., 19(3),

667 707–713, doi:10.1111/j.1523-1739.2005.00702.x, 2005.

668 Kucharik, C. J., Foley, J. A., Delire, C., Fisher, V. A., Coe, M. T., Lenters, J. D., Young-Molling,

669 C., Ramankutty, N., Norman, J. M. and Gower, S. T.: Testing the performance of a Dynamic Global

670 Ecosystem Model: Water balance, carbon balance, and vegetation structure, Global Biogeochem. Cycles,

671 14(3), 795–825, doi:10.1029/1999GB001138, 2000.

672 Lee, J. E., Frankenberg, C., van der Tol, C., Berry, J. A., Guanter, L., Boyce, C. K., Fisher, J. B.,

673 Morrow, E., Worden, J. R., Asefi, S., Badgley, G. and Saatchi, S.: Forest productivity and water stress in

674 Amazonia: observations from GOSAT chlorophyll fluorescence, Proc. R. Soc. B Biol. Sci., 280(1761),

675 20130171–20130171, doi:10.1098/rspb.2013.0171, 2013.

676   Lehmann, C. E. R., Archibald, S. A., Hoffmann, W. A. and Bond, W. J.: Deciphering the

677   distribution of the savanna biome, New Phytol., 191, 197–209, doi:10.1111/j.1469-8137.2011.03689.x,

678   2011.

679   Lehmann, C. E. R., Anderson, T. M., Sankaran, M., Higgins, S. I., Archibald, S., Hoffmann, W.

680   A., Hanan, N. P., Williams, R. J., Fensham, R. J., Felfili, J., Hutley, L. B., Ratnam, J., Jose, J. S., Montes,

681   R., Franklin, D., Russell-Smith, J., Ryan, C. M., Durigan, G., Hiernaux, P., Haidar, R., Bowman, D. M.

682   J. S., and Bond, W. J.: Savanna Vegetation-Fire-Climate Relationships Differ Among Continents,

683   Science, 343 (January), 548–553, doi:10.1126/science.1247355, 2014.

684   Long, W., Yang, X. and Donghai, L.: Patterns of species diversity and soil nutrients along a

685   chronosequence of vegetation recovery in Hainan Island, South China, Ecol. Res., 2012.

686   Malhi, Y., Aragão, L. E. O. C., Metcalfe, D. B., Paiva, R., Quesada, C. A., Almeida, S., Anderson,

687   L., Brando, P., Chambers, J. Q., da Costa, A. C. L., Hutyra, L. R., Oliveira, P., Patiño, S., Pyle, E. H.,

688   Robertson, A. L. and Teixeira, L. M.: Comprehensive assessment of carbon productivity, allocation and

689   storage in three Amazonian forests, Glob. Chang. Biol., 15, 1255–1274, doi:10.1111/j.1365-

690   2486.2008.01780.x, 2009.

691   Marengo, J. A.: Interdecadal variability and trends of rainfall across the Amazon basin, Theor.

692   Appl. Climatol., 78(1–3), 79–96, doi:10.1007/s00704-004-0045-8, 2004.

693   Marimon Junior, B. H. and Haridasan, M.: Comparação da vegetação arbórea e características

694   edáficas de um cerradão e um cerrado sensu stricto em áreas adjacentes sobre solo distrófico no leste de

695   Mato Grosso, Brasil, Acta Bot. Brasilica, 19(4), 913–926, doi:10.1590/S0102-33062005000400026,

696   2005.

697   Marimon, B. S., Lima, E. S., Duarte, T. G., Chieregatto, L. C., Ratter, J. A.: Observations on the

698   vegetation of northeastern Mato Grosso, Brazil. IV. An analysis of the Cerrado-Amazonian Forest

699   ecotone, Edinburgh Journal of Botany, 63, 323–341, doi: 10.1017/S0960428606000576, 2006.

700   Marimon, B. S., Marimon-Junior, B. H., Feldpausch, T. R., Oliveira-Santos, C., Mews, H. A.,

701   Lopez-Gonzalez, G., Lloyd, J., Franczak, D. D., de Oliveira, E. A., Maracahipes, L., Miguel, A., Lenza,

702   E. and Phillips, O. L.: Disequilibrium and hyperdynamic tree turnover at the forest–cerrado transition

703   zone in southern Amazonia, Plant Ecol. Divers., 7(1–2), 281–292, doi:10.1080/17550874.2013.818072,

704   2014.

705   Mercado, L. M., Patino, S., Domingues, T. F., Fyllas, N. M., Weedon, G. P., Sitch, S., Quesada,

706   C. A., Phillips, O. L., Aragao, L. E. O. C., Malhi, Y., Dolman, A. J., Restrepo-Coupe, N., Saleska, S. R.,

707   Baker, T. R., Almeida, S., Higuchi, N. and Lloyd, J.: Variations in Amazon forest productivity correlated

708   with foliar nutrients and modelled rates of photosynthetic carbon supply, Philos. Trans. R. Soc. Lond. B.

709   Biol. Sci., 366(1582), 3316–3329, doi:10.1098/rstb.2011.0045, 2011.

710   Morandi, P.S., Marimon-Junior, B. H., Oliveira, E. A., Reis, S. M. A., Valadão, M. B. X.,

711   Forsthofer, M., Passos, F. B., Marimon, B. S.: Vegetation Succession in the Cerrado-Amazonian Forest

712   Transition Zone of Mato Gross State, Brazil, Edinburgh Journal of Botany, 73, 83-93, doi:

713   10.1017/S096042861500027X, 2016.

714   Moreno, M. I. C., Schiavini, I. and Haridasan, M.: Fatores edáficos influenciando na estrutura de

715   fitofisionomias do cerrado, Caminhos da Geogr., 9(25), 173–194, 2008.

716   Murphy, B. P. and Bowman, D. M. J. S.: What controls the distribution of tropical forest and

717   savanna?, Ecol. Lett., 15, 748–758, doi:10.1111/j.1461-0248.2012.01771.x, 2012.

718   Myers, N., Fonseca, G. A B., Mittermeier, R. A, Fonseca, G. A. B. and Kent, J.: Biodiversity

719   hotspots for conservation priorities, Nature, 403(6772), 853–858, doi:10.1038/35002501, 2000.

720   Nardoto, G. B., Bustamante, M. M. C., Pinto, A. S. and Klink, C. A. Nutrient use efficiency at

721   ecosystem and species level in savanna areas of Central Brazil and impacts of fire, J. Trop. Ecol., 22,

722   191–201, doi:10.1017/S0266467405002865, 2006.

723   Nogueira, E. M., Yanai, A. M., Fonseca, F. O. and Fearnside, P. M.: Carbon stock loss from

724   deforestation through 2013 in Brazilian Amazonia, Glob. Chang. Biol., doi:10.1111/gcb.12798, 2015.

725   Nunes, E. L., Costa, M. H., Malhado, A. C. M., Dias, L. C. P., Vieira, S. A., Pinto, L. B. and Ladle,

726   R. J.: Monitoring carbon assimilation in South America's tropical forests: Model specification and

727   application to the Amazonian droughts of 2005 and 2010, Remote Sens. Environ., 117, 449–463,

728   doi:10.1016/j.rse.2011.10.022, 2012.

729   Oliveira, B., Marimon-Junior, B. H., Mews, H. A., Valadão, M. B. X., Marimon, B. S.: Unraveling

730   the ecosystem functions in the Amazonia–Cerrado transition: evidence of hyperdynamic nutrient cycling,

731   Plant Ecol., 218(2), 225–239, doi:10.1007/s11258-016-0681-y, 2017.

732   Oyama, M. D. and Nobre, C. A.: A new climate-vegetation equilibrium state for Tropical South

733   America, Geophys. Res. Lett., 30(23), 10–13, doi:10.1029/2003GL018600, 2003.

734   Parton, W. J., Scurlock, J. M. O., Ojima, D. S., Gilmanov, T. G., Scholes, R. J., Schimel, D. S.,

735   Kirchner, T., Menaut, J.-C., Seastedt, T., Garcia Moya, E., Kamnalrut, A. and Kinyamario, J. I.:

736   Observations and modeling of AGB and soil organic matter dynamics for the grassland biome worldwide,

737   Global Biogeochem. Cycles, 7, 785, doi:10.1029/93GB02042, 1993.

738   Pereira, M. P. S., Malhado, A. C. M. and Costa, M. H.: Predicting land cover changes in the

739   Amazon rainforest: An ocean-atmosphere-biosphere problem, Geophys. Res. Lett., 39(9),

740   doi:10.1029/2012GL051556, 2012.

741   Pires, G. F. and Costa, M. H.: Deforestation causes different subregional effects on the Amazon

742   bioclimatic equilibrium, Geophys. Res. Lett., 40(14), 3618–3623, doi:10.1002/grl.50570, 2013.

743   Quesada, C. A., Lloyd, J., Schwarz, M., Baker, T. R., Phillips, O. L., Patiño, S., Czimczik, C.,

744   Hodnett, M. G., Herrera, R., Arneth, A., Lloyd, G., Malhi, Y., Dezzeo, N., Luizão, F. J., Santos, A. J. B.,

745   Schmerler, J., Arroyo, L., Silveira, M., Priante Filho, N., Jimenez, E. M., Paiva, R., Vieira, I., Neill, D.

746   A., Silva, N., Peñuela, M. C., Monteagudo, A., Vásquez, R., Prieto, A., Rudas, A., Almeida, S., Higuchi,

747   N., Lezama, A. T., López-González, G., Peacock, J., Fyllas, N. M., Alvarez Dávila, E., Erwin, T., di Fiore,

748   A., Chao, K. J., Honorio, E., Killeen, T., Peña Cruz, A., Pitman, N., Núñez Vargas, P., Salomão, R.,

749   Terborgh, J. and Ramírez, H.: Regional and large-scale patterns in Amazon forest structure and function

750   are mediated by variations in soil physical and chemical properties, Biogeosciences Discuss., 6, 3993–

751   4057, doi:10.5194/bgd-6-3993-2009, 2009.

752   Quesada, C. A., Lloyd, J., Anderson, L. O., Fyllas, N. M., Schwarz, M. and Czimczik, C. I.: Soils

753   of Amazonia with particular reference to the RAINFOR sites, Biogeosciences, 8, 1415–1440,

754   doi:10.5194/bg-8-1415-2011, 2011.

755   Quesada, C. A., Phillips, O. L., Schwarz, M., Czimczik, C. I., Baker, T. R., Patiño, S., Fyllas, N.

756   M., Hodnett, M. G., Herrera, R., Almeida, S., Alvarez Dávila, E., Arneth, A., Arroyo, L., Chao, K. J.,

757   Dezzeo, N., Erwin, T., Di Fiore, A., Higuchi, N., Honorio Coronado, E., Jimenez, E. M., Killeen, T.,

758   Lezama, A. T., Lloyd, G., Löpez-González, G., Luizão, F. J., Malhi, Y., Monteagudo, A., Neill, D. A.,

759 Núñez Vargas, P., Paiva, R., Peacock, J., Peñuela, M. C., Peña Cruz, A., Pitman, N., Priante Filho, N.,

760 Prieto, A., Ramírez, H., Rudas, A., Salomão, R., Santos, A. J. B., Schmerler, J., Silva, N., Silveira, M.,

761 Vásquez, R., Vieira, I., Terborgh, J. and Lloyd, J.: Basin-wide variations in Amazon forest structure and

762 function are mediated by both soils and climate, Biogeosciences, 9(6), 2203–2246, doi:10.5194/bg-9-

763 2203-2012, 2012.

764 Reis, S. M., Marimon, B. S., Marimon Junior, B.-H., Gomes, L., Morandi, P. S., Freire, E. G. and

765 Lenza, E.: Resilience of savanna forest after clear-cutting in the Cerrado-Amazon transition zone,

766 Bioscience, 31(5), 1519–1529, doi:10.14393/BJ-v31n5a2015-26368, 2015.

767 Restrepo-Coupe, N., da Rocha, H. R., Hutyra, L. R., da Araujo, A. C., Borma, L. S.,

768 Christoffersen, B., Cabral, O. M. R., de Camargo, P. B., Cardoso, F. L., da Costa, A. C. L., Fitzjarrald,

769 D. R., Goulden, M. L., Kruijt, B., Maia, J. M. F., Malhi, Y. S., Manzi, A. O., Miller, S. D., Nobre, A. D.,

770 von Randow, C., S, L. D. A., Sakai, R. K., Tota, J., Wofsy, S. C., Zanchi, F. B. and Saleska, S. R.: What

771 drives the seasonality of photosynthesis across the Amazon basin? A cross-site analysis of eddy flux tower

772 measurements from the Brazil flux network, Agric. For. Meteorol., 182–183, 128–144,

773 doi:10.1016/j.agrformet.2013.04.031, 2013.

774 Rezende, A. V, Sanquetta, C. R. and Filho, F. A.: Efeito do desmatamento no estabelecimento de

775 espécies lenhosas em um cerrado Sensu stricto, Floresta, 35, 69–88, 2005.

776 Ribeiro, J. F. and Walter, B. M. T.: As Principais Fitofisionomias do bioma Cerrado, in Cerrado:

777 ecologia e flora, pp. 153–212., 2008.

778   Rocha, H. R. da, Goulden, M. L., Miller, S. D., Menton, M. C., Pinto, L. D. V. O., De Freitas, H.

779   C. and Figueira, A. M. E. S.: Seasonality of water and heat fluxes over a tropical forest in eastern

780   Amazonia, Ecol. Appl., 14(4 SUPPL.), doi:10.1890/02-6001, 2004.

781   Roy, S. B. and Avissar, R.: Impact of land use/land cover change on regional hydrometeorology

782   in Amazonia, J. Geophys. Res., 107(D20), 1–12, doi:10.1029/2000JD000266, 2002.

783   Saatchi, S., Houghton, R. A., Dos Santos Alvalá, R. C., Soares, J. V. and Yu, Y.: Distribution of

784   aboveground live AGB in the Amazon basin, Glob. Chang. Biol., 13(4), 816–837, doi:10.1111/j.1365-

785   2486.2007.01323.x, 2007.

786   Salazar, L. F., Nobre, C. A. and Oyama, M. D.: Climate change consequences on the biome

787   distribution in tropical South America, Geophys. Res. Lett., 34(April), 2–7, doi:10.1029/2007GL029695,

788   2007.

789   Senna, M. C. A., Costa, M. H., Pinto, L. I.C., Imbuzeiro, H. M. A., Diniz, L. M. F. and Pires, G.

790   F.: Challenges to reproduce vegetation structure and dynamics in Amazonia using a coupled climate-

791   biosphere model, Earth Interact., 13(11), doi:10.1175/2009EI281.1, 2009.

792   Shukla, J., Nobre, C. and Sellers, P.: Amazon deforestation and climate change, Science, 247,

793   1322–1325, doi:10.1126/science.247.4948.1322, 1990.

794   Silva, J. F., Fariñas, M. R., Felfili, J. M. and Klink, C. A.: Spatial heterogeneity, land use and

795   conservation in the cerrado region of Brazil, in Journal of Biogeography, vol. 33, pp. 536–548., 2006.

796   Silvério, D. V, Brando, P. M., Balch, J. K., Putz, F. E., Nepstad, D. C., Oliveira-Santos, C. and

797   Bustamante, M. M. C.: Testing the Amazon savannization hypothesis: fire effects on invasion of a

798 neotropical forest by native cerrado and exotic pasture grasses, Philos. Trans. R. Soc. Lond. B. Biol. Sci.,

799 368, 20120427, doi:10.1098/rstb.2012.0427, 2013.

800 Smith, B., Wärlind, D., Arneth, A., Hickler, T., Leadley, P., Siltberg, J. and Zaehle, S.:

801 Implications of incorporating N cycling and N limitations on primary production in an individual-based

802 dynamic vegetation model, Biogeosciences, 11(7), 2027–2054, doi:10.5194/bg-11-2027-2014, 2014.

803 Thompson, S. L. and Pollard, D.: A global climate model (GENESIS) with a land-surface transfer

804 scheme (LSX). Part I: present climate simulation, J. Clim., 8, 732–761, doi:10.1175/1520-

805 0442(1995)008<0732:AGCMWA>2.0.CO;2, 1995.

806 Torello-Raventos, M., Feldpausch, T., Veenendaal, E., Schrodt, F., Saiz, G., Domingues, T.,

807 Djagbletey, G., Ford, A., Kemp, J., Marimon, B., Hur Marimon Junior, B., Lenza, E., Ratter, J.,

808 Maracahipes, L., Sasaki, D., Sonké, B., Zapfack, L., Taedoumg, H., Villarroel, D., Schwarz, M., Quesada,

809 C., Yoko Ishida, F., Nardoto, G., Affum-Baffoe, K., Arroyo, L., Bowman, D., Compaore, H., Davies, K.,

810 Diallo, A., Fyllas, N., Gilpin, M., Hien, F., Johnson, M., Killeen, T., Metcalfe, D., Miranda, H., Steininger,

811 M., Thomson, J., Sykora, K., Mougin, E., Hiernaux, P., Bird, M., Grace, J., Lewis, S., Phillips, O. and

812 Lloyd, J.: On the delineation of tropical vegetation types with an emphasis on forest/savanna transitions,

813 Plant Ecol. Divers., 6, 101–137, doi:10.1080/17550874.2012.76281, 2013.

814 Valadão, M. B. X., Marimon-Junior, B. H., Oliveira, B., Lúcio, N. W., Souza, M. G. R., Marimon,

815 B. S.: AGB hyperdynamic as a key modulator of forest self-maintenance in dystrophic soil at Amazonia-

816 Cerrado transition. Scientia Forestalis, 44, 475-485, 2016.

817 Veenendaal, E. M., Torello-Raventos, M., Feldpausch, T. R., Domingues, T. F., Gerard, F.,

818 Schrodt, F., Saiz, G., Quesada, C. A., Djagbletey, G., Ford, A., Kemp, J., Marimon, B. S., Marimon-

819 Junior, B. H., Lenza, E., Ratter, J. A., Maracahipes, L., Sasaki, D., Sonk, B., Zapfack, L., Villarroel, D.,

820 Schwarz, M., Yoko Ishida, F., Gilpin, M., Nardoto, G. B., Affum-Baffoe, K., Arroyo, L., Bloomfield, K.,

821 Ceca, G., Compaore, H., Davies, K., Diallo, A., Fyllas, N. M., Gignoux, J., Hien, F., Johnson, M., Mougin,

822 E., Hiernaux, P., Killeen, T., Metcalfe, D., Miranda, H. S., Steininger, M., Sykora, K., Bird, M. I., Grace,

823 J., Lewis, S., Phillips, O. L. and Lloyd, J.: Structural, physiognomic and above-ground AGB variation in

824 savanna-forest transition zones on three continents - How different are co-occurring savanna and forest

825 formations?, Biogeosciences, 12(10), 2927–2951, doi:10.5194/bg-12-2927-2015, 2015.

826 Verberne, E. L. J., Hassink, J., De Willigen, P., Groot, J. J. R. and Van Veen, J. A.: Modelling

827 organic matter dynamics in different soils, Netherlands J. Agric. Sci., 38, 221–238, 1990.

828 Vourlitis, G. L., de Lobo, F. A., Lawrence, S., de Lucena, I. C., Pinto, O. B., Dalmagro, H. J.,

829 Ortiz, C. E. and de Nogueira, J. S.: Variations in Stand Structure and Diversity along a Soil Fertility

830 Gradient in a Brazilian Savanna (Cerrado) in Southern Mato Grosso, Soil Sci. Soc. Am. J., 77(4), 1370–

831 1379, doi:10.2136/sssaj2012.0336, 2013.

832 Wang, S., Huang, J., He, Y. and Guan, Y.: Combined effects of the Pacific Decadal Oscillation

833 and El Niño-Southern Oscillation on Global Land Dry–Wet Changes, Sci. Rep., 4, 6651,

834 doi:10.1038/srep06651, 2014.

835 Yang, X. and Post, W. M.: Phosphorus transformations as a function of pedogenesis: A synthesis

836 of soil phosphorus data using Hedley fractionation method, Biogeosciences, 8, 2907–2916,

837 doi:10.5194/bg-8-2907-2011, 2011.

838 Yang, X., Post, W. M., Thornton, P. E. and Jain, A.: The distribution of soil phosphorus for global

839 biogeochemical modeling, Biogeosciences, 10, 2525–2537, doi:10.5194/bg-10-2525-2013, 2013.

840   Yang, X., Thornton, P. E., Ricciuto, D. M. and Post, W. M.: The role of phosphorus dynamics in

841   tropical forests - A modeling study using CLM-CNP, Biogeosciences, 11, 1667–1681, doi:10.5194/bg-

842   11-1667-2014, 2014.

843

844

845
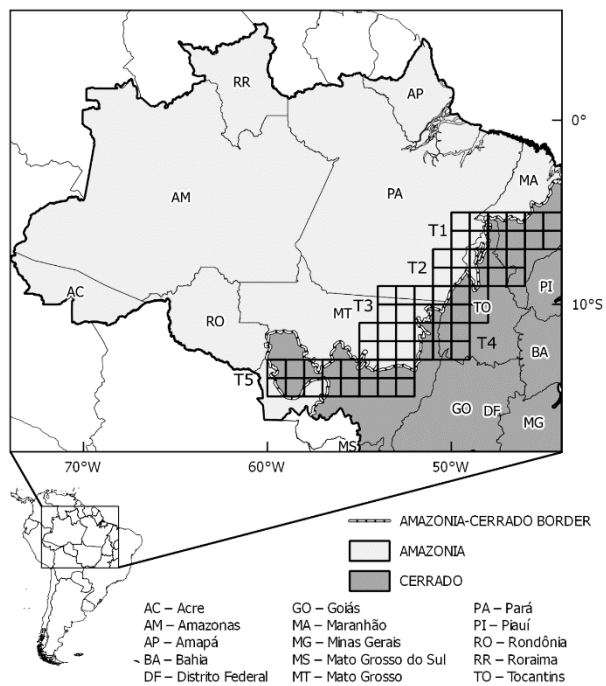
Figure 1. Delimitation of the study area Amazonia (in light gray) and Cerrado (in dark gray) (IBGE, 2004), and the location of five transects used in this work (from T1 to T5). The dashed line represents the border between biomes.
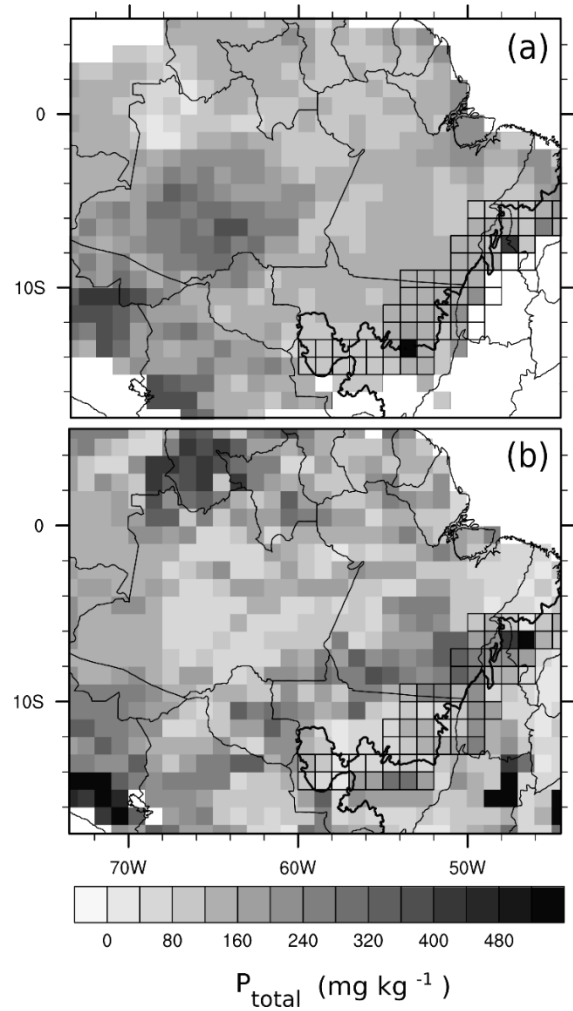
849

850 **Figure 2.** (a) Map of regional total P in the soil (PR), (b) Map of global total P in the soil (Yang et al.,

851 2013) (PG).

852
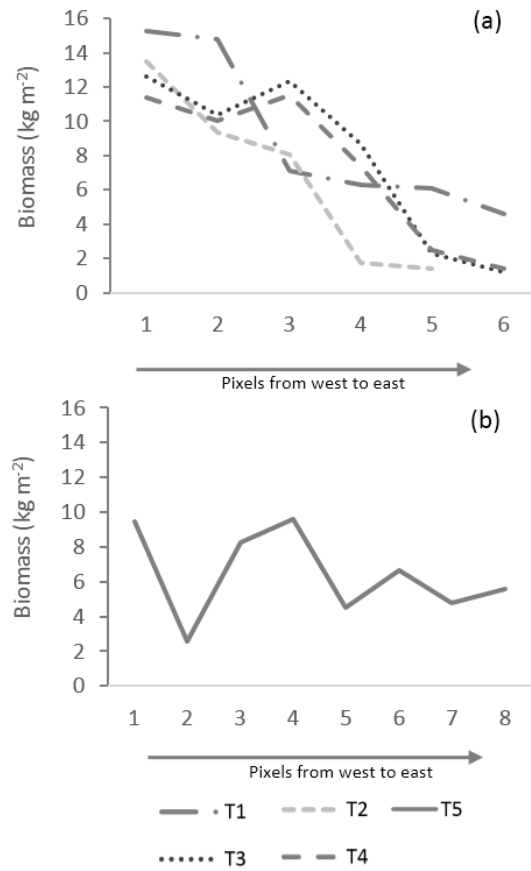
853

854   **Figure 3.** Average variations of AGB in pixels from West to East in the Amazonia-Cerrado transition

855   for transects T1, T2, T3 and T4 (a), and T5 (b).

856
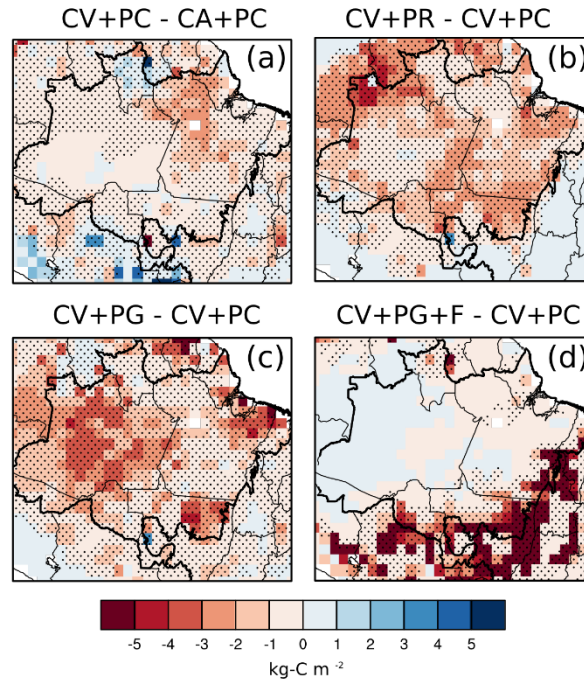
Figure 4. Effects of inter-annual climate variability (a), Regional P limitation (b), Global P limitation (c),

and fire (d) on AGB. The hatched areas indicate that the variables are significantly different compared to

the control simulation at the level of 95% according to the t-test. The thick black line is the geographical

limits of the biomes.

861
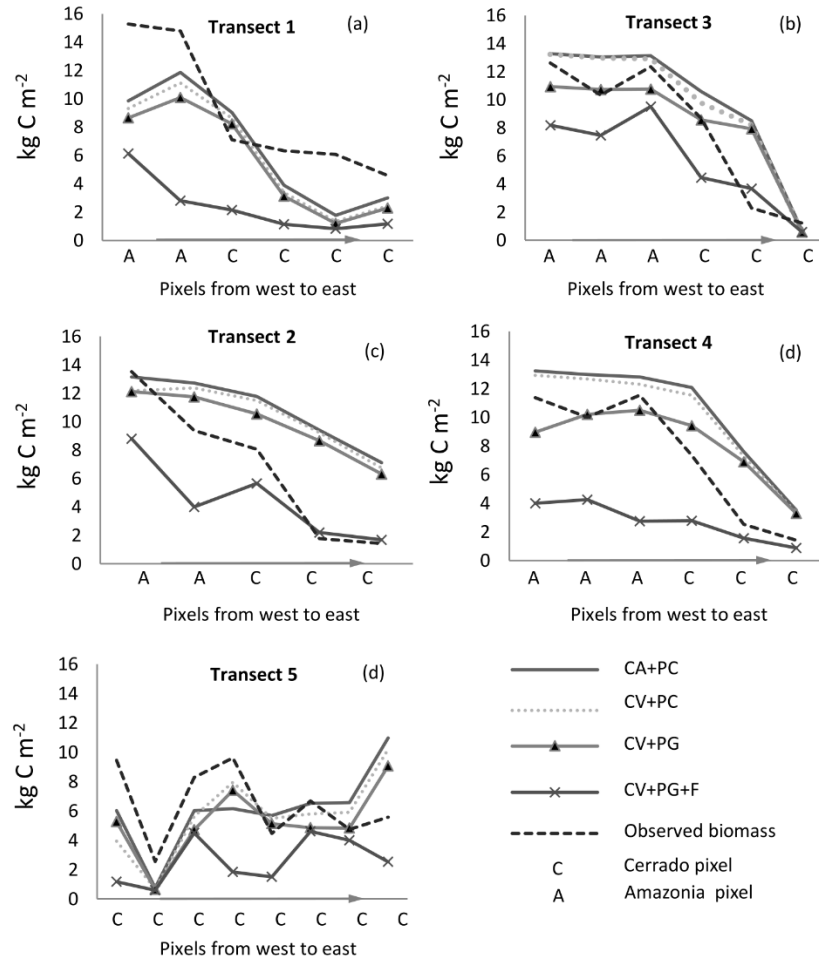
Figure 5. Average longitudinal AGB gradient in Amazonia-Cerrado transition simulated for T1 to T5 considering different combinations: observed data; seasonal climate control simulation (CA+PC); inter-annual climate variability (CV+PC); inter-annual climate variability + global P limitation (CV+PG); and inter-annual climate variability + P + fire occurrence (CV+PG+F).
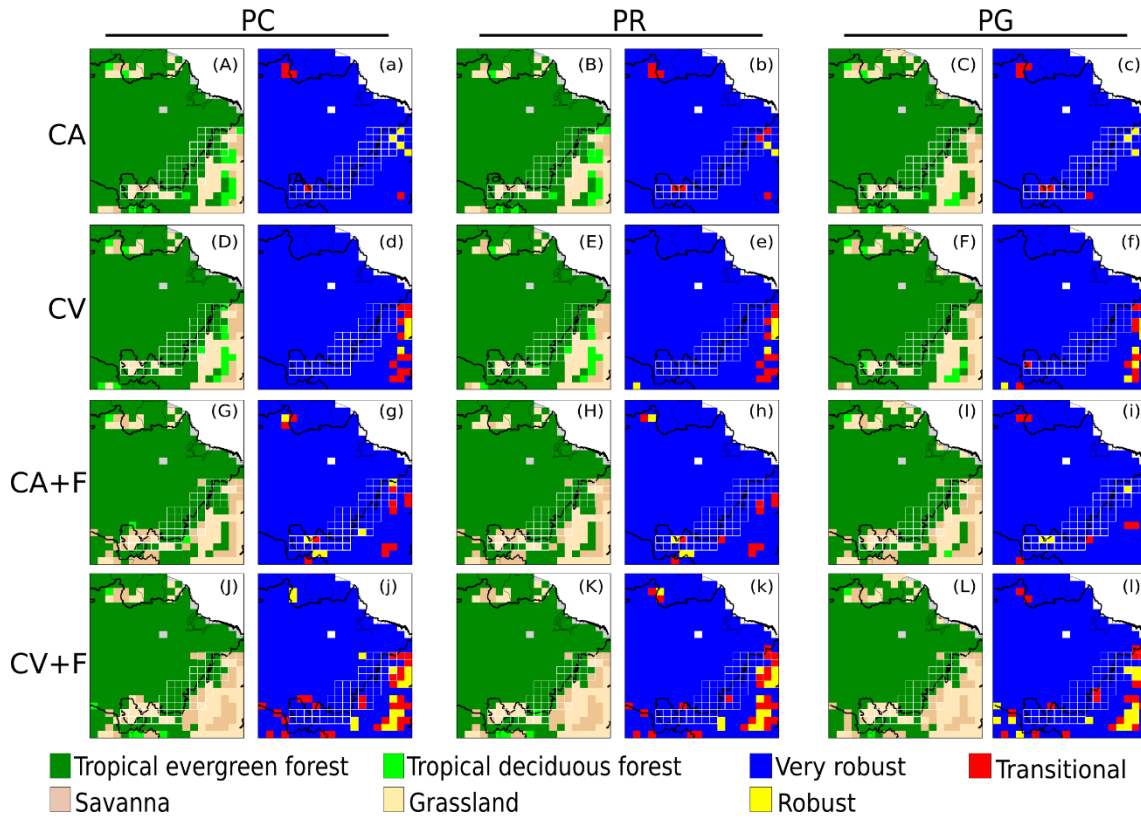
Figure 6. Results for the dominant vegetation cover simulated by INLAND for the different treatments (A-L) and a metric of variability of results (a-l). Simulations are considered very robust if the dominant vegetation agrees on 9-10 of the last 10 years of simulation, robust if it agrees on 7-8 years, and transitional if on 6 or fewer years.

874 **Table 1.** Simulations with different scenarios evaluated by INLAND model in Amazonia-Cerrado

875 transition. CA, climatological average, 1961-1990; CV, monthly climate data, 1948-2008; the nutrient

876 limitation on V_{max} - PC, no P limitation ($V_{max} = 65$ μmol-CO_2 m^{-2} s^{-1}); PR, regional P limitation; PG,

877 global P limitation).

			V_{max}		
Climate	**CO$_2$**	**Fire (F)**	**PC**	**PR**	**PG**
CA	Variable	Off	CA+PC	CA+PR	CA+PG
CA	Variable	On	CA+PC+F	CA+PR+F	CA+PG+F
CV	Variable	Off	CV+PC	CV+PR	CV+PG
CV	Variable	On	CV+PC+F	CV+PR+F	CV+PG+F

878

879

880 **Table 2.** Individual and combined effects for each simulation in Amazonia-Cerrado transition. CA,

881 climatological seasonal average, 1961-1990; CV, monthly climate data, 1948-2008; the nutrient limitation

882 on V_{max} - PC, no P limitation ($V_{max} = 65$ μmolCO$_2$ m^{-2} s^{-1}); PR, regional P limitation; PG, global P

883 limitation)

Climate (C)	Phosphorus (P)	Fire (F)
(CV+PC)-(CA+PC)	(CA+PR)-(CA+PC)	(CA+PC+F)-(CA+PC)
(CV+PR)-(CA+PR)	(CV+PR)-(CV+PC)	(CV+PC+F)-(CV+PC)
(CV+PG)-(CA+PG)	(CA+PG)-(CA+PC)	(CA+PR+F)-(CA+PR)
	(CV+PG)-(CV+PC)	(CV+PR+F)-(CV+PR)
		(CA+PG+F)-(CA+PG)
		(CV+PG+F)-(CV+PG)

884

885

886 **Table 3.** Summary of average NPP, LAI and AGB for the Amazonia-Cerrado transition at the transects

887 domains, considering all simulations with CA and CV regardless of fire presence or P limitation. The

888 results of a one-way ANOVA are also shown, including the F statistic, and p value. Values within each

889 column followed by a different letter are significantly different ($p < 0.05$) according to the Tukey–Kramer

890 test (n=1860: 31 pixels x 10 years x $n_{simulation/2}$).

Group 1	NPP		LAI$_{total}$		LAI$_{lower}$		LAI$_{upper}$		AGB	
	kg-C m^{-2} yr^{-1}		m^2 m^{-2}		m^2 m^{-2}		m^2 m^{-2}		kg-C m^{-2}	
CA	0.68	a	7.47	a	1.98	a	5.49	a	6.68	a
CV	0.64	b	7.15	b	2.11	a	5.04	b	6.30	b
F	*40.2*		*57.2*		*2.96*		*36.0*		*11.3*	
p	*<0.001*		*<0.001*		*ns*		*<0.01*		*<0.001*	

891

892

893 **Table 4.** Summary of average NPP, LAI and AGB for the transition at the transects domains, considering

894 different P limitation, regardless of climate and fire presence. The results of a one-way ANOVA are also

895 shown, including the F statistic, and p value. Values within each column followed by a different letter are

896 significantly different ($p < 0.05$) according to the Tukey–Kramer test (n=1240: 31 pixels x 10 years x

897 $n_{simulation/3}$).

Group 2	NPP		LAI_{total}		LAI_{lower}		LAI_{upper}		AGB	
	kg-C m^{-2} yr^{-1}		m^2 m^{-2}		m^2 m^{-2}		m^2 m^{-2}		kg-C m^{-2}	
PC	0.71	a	7.64	a	1.84	b	5.80	a	7.15	a
PR	0.64	b	7.15	b	2.19	a	4.95	b	6.20	b
PG	0.64	b	7.14	b	2.10	a	5.04	b	6.12	b
$F_{2.99}$	62.8		61.0		8.75		53.5		33.6	
p	<0.001		<0.001		<0.01		<0.01		<0.001	

898

899

900 **Table 5.** Summary of average NPP, LAI and AGB for the transition at the transects domains, considering

901 presence or absence of fire. The results of a one-way ANOVA are also shown, including the F statistic,

902 and p value. Values within each column followed by a different letter are significantly different ($p < 0.05$)

903 according to the Tukey–Kramer test (n=1860: 31 pixels x 10 years x $n_{simulation/2}$).

Group 3	NPP		LAI_{total}		LAI_{lower}		LAI_{upper}		AGB	
	kg-C m^{-2} yr^{-1}		m^2 m^{-2}		m^2 m^{-2}		m^2 m^{-2}		kg-C m^{-2}	
Fire OFF	0.66	a	6.72	b	0.88	b	5.84	a	8.47	b
Fire ON	0.67	b	7.90	a	3.21	a	4.69	b	4.51	a
$F_{3.84}$	8.28		937		1459		249		1719	
p	<0.005		<0.001		<0.01		<0.01		<0.001	

904

905

906 **Table 6.** Summary of average NPP, LAI and AGB for the transition at the transects domains, considering

907 all factor combinations. The results of a one-way ANOVA are also shown, including the F statistic, and

908 p value. Values within each column followed by a different letter are significantly different ($p < 0.05$)

909 according to the Tukey–Kramer test (n=310: 31 pixels x 10 years).

	NPP		**LAI$_{total}$**		**LAI$_{lower}$**		**LAI$_{upper}$**		**AGB**	
	kg-C m^{-2} yr^{-1}		m^2 m^{-2}		m^2 m^{-2}		m^2 m^{-2}		kg-C m^{-2}	
CV+PC	0.69	bcd	6.96	d	0.84	e	6.48	a	9.01	ab
CV+PG	0.61	f	6.24	f	0.85	e	5.60	bc	7.91	c
CV+PR	0.62	f	6.33	f	0.85	e	5.74	bc	8.04	c
CV+PC+F	0.69	abc	7.92	b	2.91	cd	4.61	ef	4.89	de
CV+PG+F	0.63	ef	7.76	b	3.73	a	5.81	bc	3.91	f
CV+PR+F	0.63	ef	7.65	bc	3.47	ab	4.69	ef	4.02	f
CA+PC	0.72	ab	7.39	c	0.91	e	6.12	ab	9.31	a
CA+PG	0.64	def	6.64	e	0.91	e	5.40	cd	8.22	c
CA+PR	0.65	cdef	6.72	de	0.91	e	5.49	cd	8.31	bc
CA+PC+F	0.74	a	8.29	a	2.69	d	5.02	de	5.40	d
CA+PG+F	0.67	cde	7.90	b	3.29	abc	4.04	g	4.45	ef
CA+PR+F	0.67	cde	7.88	b	3.19	bc	4.18	fg	4.42	ef
F	16.2		115		140		38.1		172	
p	<0.001		<0.001		<0.01		<0.01		<0.001	

910

911   **Table 7**. Correlation coefficients of AGB simulated by INLAND and field estimates (n= 310: 31 pixels

912   x 10 years).

	T1	**T2**	**T3**	**T4**	**T5**	**All transects**
CA+PC	0.843	0.928	0.886	0.937	0.337	0.786
CV+PC	0.838	0.884	0.890	0.939	0.355	0.781
CA+PR	0.793	0.848	0.830	0.911	0.399	0.756
CV+PR	0.795	0.793	0.832	0.907	0.527	0.771
CA+PG	0.814	0.951	0.838	0.889	0.388	0.776
CV+PG	0.825	0.922	0.840	0.879	0.496	0.792
CA+PC+F	0.988	0.987	0.977	0.892	0.133	0.795
CV+PC+F	0.976	0.947	0.933	0.908	0.187	0.790
CA+PR+F	0.842	0.805	0.981	0.808	0.561	0.799
CV+PR+F	0.925	0.804	0.927	0.808	0.319	0.757
CA+PG+F	0.844	0.961	0.980	0.830	0.430	0.809
CV+PG+F	0.845	0.932	0.931	0.881	0.177	0.753
CA avg	0.854	0.913	0.915	0.878	0.375	0.787
CV avg	0.867	0.880	0.892	0.887	0.344	0.774

913